Electronic structure of Sn/Si(111)-($\sqrt{3}\times\sqrt{3}$)$R30°$ as a function of Sn coverage

J. Lobo,[1] A. Tejeda,[1] A. Mugarza,[2] and E. G. Michel[1,3]
[1]*Departamento de Física de la Materia Condensada, Universidad Autónoma de Madrid, 28049 Madrid, Spain*
[2]*Donostia International Physics Center and Centro Mixto de Materiales CSIC/UPV, Universidad del Pais Vasco, San Sebastián, Spain*
[3]*Instituto Universitario de Ciencia de Materiales "Nicolás Cabrera," Universidad Autónoma de Madrid, 28049 Madrid, Spain*
(Received 1 July 2003; revised manuscript received 7 October 2003; published 31 December 2003)

We report an investigation of the electronic band structure of the $Si_xSn_{(1-x)}/Si(111)-(\sqrt{3}\times\sqrt{3})R30°$ solid solution using angle-resolved photoemission. This reconstruction was studied in the coverage range between 0.15 and 0.40 monolayers at room and low temperature, with special emphasis on the analysis of the symmetry and morphology of the surface states and the metallic character as a function of temperature and coverage. While there is no indication of a (3×3) pattern at low temperature with structural techniques, strikingly clear features of this phase are found in the valence band analysis for a coverage of 0.33 ML. We present also an analysis of the influence of the Si intermixing in the surface-state behavior and metallic character.

DOI: 10.1103/PhysRevB.68.235332 PACS number(s): 73.20.At, 79.60.−i

I. INTRODUCTION

The properties of ordered metal overlayers on semiconducting substrates have been investigated for many years, due to both their fundamental interest and their many implications in several technologically relevant fields.[1–3] One of the most common adsorbate-induced surface reconstructions is the ($\sqrt{3}\times\sqrt{3}$)$R30°$ (in the following $\sqrt{3}$), which is found on the (111) surfaces of Si and Ge for many different metals. The $\sqrt{3}$ reconstruction for Sn and Pb on Si(111) and Ge(111) is observed for coverages around 1/3 monolayer (ML) of adsorbate atoms, which occupy all available T_4 surface sites.[4,5] This phase has received renewed attention since the discovery of a temperature-induced phase transition to a low-temperature (LT) (3×3) phase for Pb/Ge(111).[6] An analogous phase transition was found soon after for Sn/Ge(111) (Ref. 7) and later on for Pb/Si(111) (Refs. 8 and 9). Several different models have been put forward to explain the origin of these phase transitions. The complementarity between occupied and unoccupied states in scanning tunneling microscope (STM) pictures suggested the formation of a surface charge density wave[6,7] (SCDW) triggered by Fermi surface nesting in the case of Pb/Ge(111) (Ref. 6) or by correlation effects in Sn/Ge(111) (Ref. 7). Later on it was reported that defects may play an important role in the phase transition,[10] since (3×3) patches are nucleated around surface defects even at room temperature (RT). As further experiments with different techniques were being performed to explore the properties of Sn/Ge(111), increasing doubts were cast about the SCDW model. No Fermi surface nesting was found in photoemission,[11] and an analysis of the electronic band structures and of the Sn $4d$ core level at RT and LT did not reveal any significant difference.[12,13] The surface band crossing the Fermi energy is split in two different surface state bands, and the Sn $4d$ core level exhibits also two components in both phases. Surface x-ray diffraction showed that both (3×3) phases for Pb/Ge(111) (Ref. 14) and Sn/Ge(111) (Refs. 15 and 16) are corrugated, and there are two kinds of Sn or Pb atoms in the unit cell, with different heights [one atom up and two down per (3×3) unit cell]. This feature explains both the two components in the Sn $4d$ core level (which appear in an approximate 1:2 proportion) and the surface band splitting. The dynamical fluctuations model[12] was proposed to explain how both features survive in the $\sqrt{3}$ phase. Molecular dynamics *ab initio* calculations[12,17,18] indicate that the adsorbate atoms vibrate rapidly at RT between the two vertical positions. While the local (3×3) ordering is preserved during times of the order of ps, the long-range order is lost due to the vertical fluctuations, and a $\sqrt{3}$ phase is observed at RT. The vertical vibrations are frozen at LT, giving rise to the (3×3) phase. The stability of the (3×3) phase has been recently related to the softening of a surface phonon,[19] which has been observed experimentally.[20]

The $\sqrt{3}$ reconstruction is stable for a rather broad coverage range in the case of Sn/Si(111) (Refs. 21 and 22)—namely, from 0.16 to 0.33 ML. This wide range is made possible by the intermixing of Si and Sn atoms at the top layer occupying all T_4 positions, forming an adatom solid solution. The surface phase is thus better described as $Si_xSn_{(1-x)}/Si(111)-(\sqrt{3}\times\sqrt{3})R30°$ $(0.5<x<0)$. The intermixed Si atoms help to form a hexagonal array with one adatom (Sn or Si) per unit cell.[23] Thus, Si atoms complete the T_4 vacancies left by the lack of Sn adatoms to form the $\sqrt{3}$ structure for coverages below 0.33 ML. It is a common practice to name the two limiting cases of the $\sqrt{3}$ reconstruction as γ or mosaic phase for a coverage of 0.16 ML, where we reach half intermixing ($x=0.5$), and α for the ideal coverage of 0.33 ML, where there is nearly no intermixing ($x\simeq0$) and a very small number of defects (3%).[21,24]

An interesting feature of Sn/Si(111) with respect to the Sn/Ge(111) case is that no phase transition has been found so far with structural techniques like low-energy electron diffraction (LEED) or STM,[25–27] besides the formation of local (3×3) patches around defect sites. However, many other electronic properties are similar to the Sn/Ge(111) system, as the existence of two components in the Sn $4d$ core level.[25,28] We may expect that the partial intermixing of Si adatoms should affect the Sn core-level line shape. Indeed, the depen-

dence of the two components with Sn coverage has been recently investigated in detail.[26] It was found that intermixed Si atoms preferentially substitute only one of the species of Sn atoms: namely, the dominating one [corresponding to a maximum of 0.22 ML—i.e., two Sn atoms per (3×3) unit cell].

Another interesting question is the metallic behavior of the system as a function of Sn coverage. In principle, a single tetravalent atom per unit cell should give rise to a metallic surface for all Sn coverages. Theoretical *ab initio* calculations predict a partial charge transfer between Sn and Si atoms, associated to a structural deformation.[21,29] This effect could give rise to a semiconducting phase for $x=0.5$ (mosaic phase), preceding the metallic α phase. Thus a semiconductor-to-metal transition would take place at intermediate coverages. Inverse photoemission studies support this idea[21] and suggest that the behavior of Sn/Si(111) might be much more complex than expected, with significant correlation effects in the unoccupied band structure of the system. A recent *ab initio* study[30] has predicted even more drastic features for these surfaces: besides a semiconducting character for the mosaic phase, decoupled surface bands associated either with Si or Sn atoms should be observed, with a strong coverage dependence in the range of the solid solution ($0.16\ \text{ML}<\Theta<0.33\ \text{ML}$). The stability and appearance of other structural configurations besides the established structure with one Sn atom up and two down (configuration 1U) have been also analyzed within the local density approximation (configurations 2U and 3U).[31]

In this paper we set out to investigate the surface electronic bands by using angle-resolved photoemission as a function of Sn coverage, in order to check their nature and evolution with coverage. The metallic character is determined from the photoemission intensity at the Fermi energy and band dispersion as a function of Sn coverage. The results are compared with theoretical predictions (band decoupling, intermediate semiconducting phase).[17,18,21,30,31]

II. EXPERIMENT

The photoemission experiments have been performed in an ultrahigh-vacuum (UHV) chamber, with a base pressure of 3×10^{-11} mbar, using synchrotron radiation light from the F2.2 beamline at HASYLAB (Hamburg, Germany). The chamber is equipped with a LEED apparatus, a quartz crystal microbalance, and an angle-resolving hemispherical electron analyzer. An overall energetic resolution of 110 meV at 21 eV and angular resolution of 0.5° was available.

The Si(111) substrate was cut from a commercial *n*-type (P-doped, $\rho=2.0$–$6.0\ \Omega$ cm) Si(111) wafer. It was cleaned using standard procedures until a (7×7) LEED pattern with low background was observed. The quality of the reconstruction was checked by monitoring the intensity of the (7×7) surface states along the $[10\bar{1}]$ direction ($\overline{\Gamma K}_{(1\times1)}$) using angle-resolved photoemission spectroscopy (ARUPS).[32] Sn was evaporated from a previously calibrated Knudsen cell with the sample held at RT. The Sn coverage (Θ_{Sn}) was calibrated both from the reading of the quartz microbalance and from the evaporation time. The values obtained were cross-checked with the intensity of the dangling bond surface state as a function of coverage[25] and with the reported stability range for the $\sqrt{3}$ phase. We estimate an accuracy of 5% in the quoted values of the coverage.[11,12] The surface was then annealed to 650 °C to favor the formation of the $\sqrt{3}$ structure. This annealing temperature gives rise to the lowest defect density at the surface, around 3%.[22] It was carefully determined using a calibrated infrared pyrometer. The photoemission intensity was normalized to the photon flux. The sample temperature during the measurements was RT and 170 K.

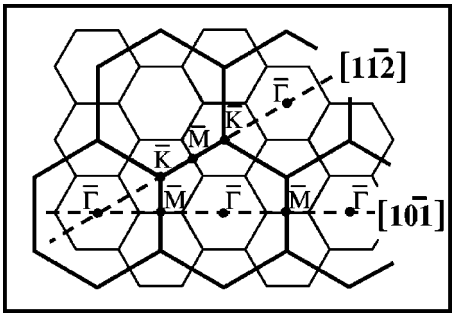

FIG. 1. Reciprocal space of the $\sqrt{3}$ (bold lines) and (3×3) (thin lines) structures. High-symmetry directions are shown as dashed lines. The lettering refers to the symmetry points of the $\sqrt{3}$ structure.

III. RESULTS AND DISCUSSION

The electronic band structure of the Sn/Si(111) interface was determined at RT and LT (170 K) along the $\overline{\Gamma K}$ and $\overline{\Gamma M}$ high-symmetry directions of the $\sqrt{3}$ first Brillouin zone (see Fig. 1) using 12.5 eV and 21 eV photons. The whole coverage range where a $\sqrt{3}$ reconstruction is observed was probed. This corresponds approximately to coverages from 0.15 ML to 0.40 ML.[4,21]

A. α-Sn/Si(111)-$(\sqrt{3}\times\sqrt{3})R30°$ phase

The α phase of Sn/Si(111) is obtained for 0.33 ML coverage (see above). We expect a small number of defects ($\sim3\%$) and residual Si intermixing only. Figure 2 (top) shows the normalized photoemission intensity distribution of the valence band in reciprocal space, probed along the two high-symmetry lines (see Fig. 1) with $h\nu=12.5$ eV at 170 K. In a simple picture, each Sn adatom in a T_4 site is bonded to the three Si atoms underneath. We expect three fully occupied backbonds and one half-filled bond per Sn adatom, giving rise to two different surface bands: one fully occupied and another one crossing the Fermi energy. The surface should be metallic. As previously reported for Sn/Si(111) (Refs. 25, 33, and 34) and for Sn,Pb/Ge(111) (Refs. 11–13) these two main surface state bands are detected along the two high-symmetry directions (see Fig. 2, top). The first surface band appears at a binding energy (BE) of 1–2 eV and it is associated with the fully occupied backbonds of Sn adatoms. The second surface band has a BE smaller than 0.5 eV and it comes from the half-occupied bond.

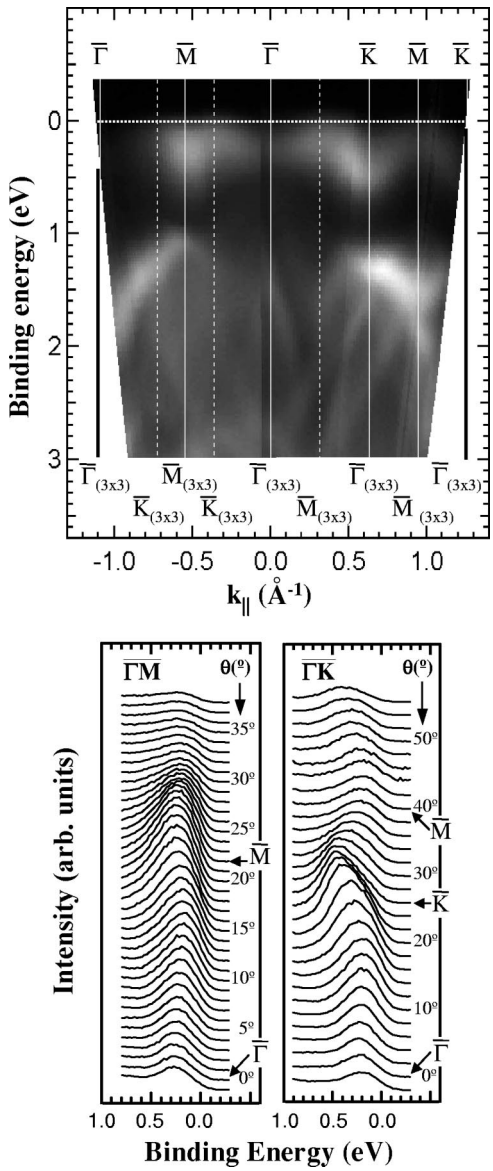

FIG. 2. Electronic bands for the α-Sn/Si(111)-($\sqrt{3}\times\sqrt{3}$)$R30°$ phase ($\Theta_{Sn}=0.33$ ML, $h\nu=12.5$ eV, 170 K). Top: binding energy vs parallel momentum for the surface bands closer to the Fermi energy. The gray scale corresponds to the normalized photoemission intensity, where darker color represents less emission. Symmetry points of the $\sqrt{3}$ (solid lines) and (3×3) phase (dashed lines) are shown in the upper and lower axes, respectively. Bottom: selected photoemission spectra showing the energy range closer to the Fermi energy as a function of emission angle along the two high-symmetry directions. Symmetry points for the $\sqrt{3}$ phase (at the Fermi energy) are shown in the spectra.

Figure 2 (bottom) shows two series of energy distribution curves (EDC's), zoomed in from the top part of Fig. 2, but shown as a function of emission angle, referred to the sample normal, along the two high-symmetry directions. The broad peak observed corresponds to the dangling bond surface state of the Sn adatoms. The intensity is higher in the first Brillouin zone and it decreases as we progress along the second. The dispersion of the half-occupied surface state is more pronounced along the $\overline{\Gamma K}$ direction. It presents maximum

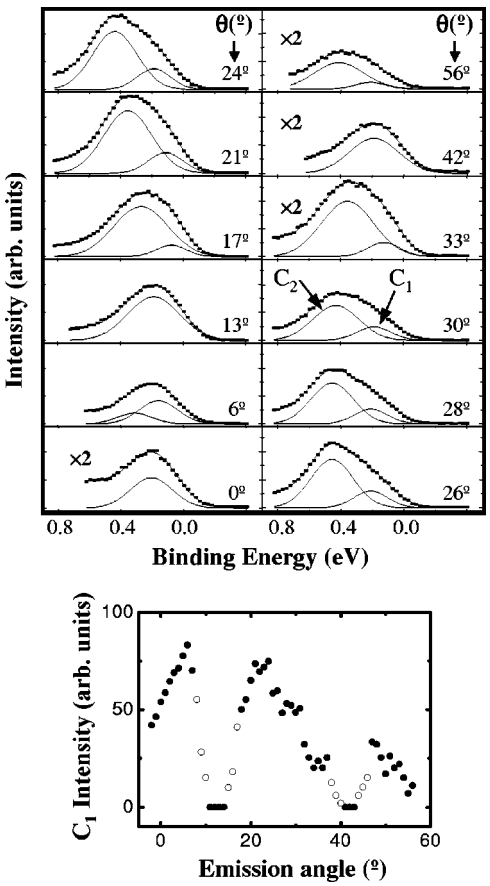

FIG. 3. Top: χ^2 line shape deconvolution of selected normalized photoemission spectra (dots) as a function of emission angle along the $\overline{\Gamma K}$ direction ($\Theta_{Sn}=0.33$ ML, $h\nu=12.5$ eV, 170 K). Solid lines represent the result of the fitting and the two components used, labeled C_1 and C_2 (the background is not shown for clarity). Some spectra could be fitted with only one component. Bottom: intensity of C_1 component as a function of emission angle (solid and open circles). Open circles are used for emission angles where the BE of C_1 is closer to the Fermi energy than our energetic resolution. Solid circles with zero intensity (for emission angles around 13° and 42°) indicate that the best fit was obtained with only one component (C_2).

intensity near the $\overline{K}$ point, which corresponds to the bottom of the surface band BE. An inspection of the line shape of the surface peak along the $\overline{\Gamma K}$ direction suggests the existence of two different components.[25] This is more clearly seen in Fig. 3 (top), where selected spectra have been represented in an enlarged energy scale. In order to understand the properties of the two split states, we performed a χ^2 line shape deconvolution of the spectra. We used two components (labeled C_1 and C_2 in Fig. 3) with a Gaussian line shape, convoluted with a Fermi function, broadened due to temperature effects and the apparatus resolution,[13] plus a suitable background. This deconvolution procedure was repeated for the different Sn coverages in the two symmetry directions at RT and LT.

Figure 3 (top) gives an example of the fitting accuracy. Normalized spectra are shown together with the fitting for selected angles along the $\overline{\Gamma K}$ direction. The quality of the

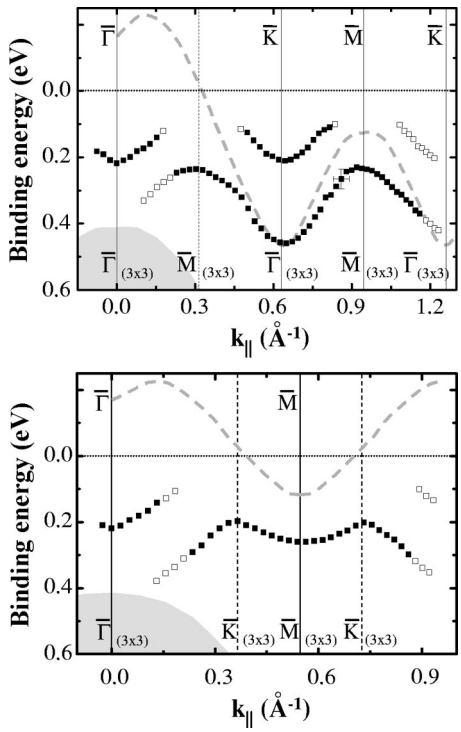

FIG. 4. Binding energy of C_1 and C_2 components (see Fig. 3) of the surface band vs parallel momentum ($\Theta_{Sn}=0.33$ ML, $h\nu=12.5$ eV, 170 K), along $\overline{\Gamma K}$ (top) and $\overline{\Gamma M}$ (bottom) directions. Solid (open) points correspond to intense (weak) components (Ref. 35). Dashed gray lines represent the expected dispersion for a half-occupied surface state in a $\sqrt{3}$ reconstruction (Ref. 36). Symmetry points of the $\sqrt{3}$ [(3×3)] phase are shown in the top (bottom) axis. Shaded areas correspond to the projection of the Ge(111) bulk bands.

fitting is quite good. The average widths are 0.22 eV (higher BE component) and 0.15 eV (lower BE component). These relatively large widths are above our resolution, indicating that they are an intrinsic property of the surface bands. Even larger widths ($\sim$230–300 meV) have been found in the parent system Sn/Ge(111).[12,13] The position and intensity of both components change visibly with emission angle. The BE's are represented in Fig. 4 versus parallel momentum along both high-symmetry directions. Some spectra can be fitted using only one component.[35] The intensity of C_1 is represented in the bottom panel of Fig. 3 versus emission angles. Open circles denote a range where the Fermi function cuts off part of the intensity, which diminishes strongly in the vicinity of 13° and 42° emission angles, both values close to $\overline{M}_{(3\times3)}$ points. Indeed, in these ranges the best fit is obtained using a single component (C_2). In view of the dispersion and intensity distribution shown in Figs. 3 and 4, we conclude that C_1 crosses the Fermi energy in several cases (e.g., around $\overline{M}_{(3\times3)}$ points along $\overline{\Gamma K}$ or around $\overline{M}$ along $\overline{\Gamma M}$). In the area close to normal emission ($\overline{\Gamma}$ point) there is no Fermi level crossing, but we detect a strong attenuation of the high BE component, which we attribute to a mixture with bulk states in this range. A similar result was obtained at RT and with a photon energy of 21 eV (not shown). The band splitting found cannot be explained assuming a conventional, flat $\sqrt{3}$ structure where Sn atoms occupy equivalent T_4 sites. The surface state expected in this kind of structure is shown as a dashed gray line in Fig. 4.[36] Besides the existence of the split component, another significant difference between the experimental data and the prediction for a flat $\sqrt{3}$ phase is the detection of surface-state intensity at the $\overline{\Gamma}$ point (normal emission). Note that the $\sqrt{3}$ surface state lies above the Fermi energy at $\overline{\Gamma}$. The intensity detected in the experiment reflects an underlying (3×3) periodicity, since it can be explained only from a (3×3) band folding, observed in this surface with much more intensity than on Sn/Ge(111).[11–13,25] This explanation agrees well with the symmetry that the two components exhibit: along both directions the two surface-state components follow the (3×3) symmetry, and not the $\sqrt{3}$ one, as we might expect from the $\sqrt{3}$ LEED pattern.

The surface band splitting found and the (3×3) symmetry of the two surface states can be easily interpreted in the dynamical fluctuations model. The existence of vertical fluctuations with (3×3) local symmetry gives rise to two kinds of Sn atoms in the unit cell and a surface band associated with each of them (see Ref. 29 for a theoretical calculation). The split band with higher BE, which is fully occupied with two electrons, has an orbital content coming mainly from the Sn atom displaced upwards, which receives charge from the other two Sn atoms displaced downwards. These two atoms are the origin of the (partially occupied) lower BE band, with only one electron in total, and of an additional unoccupied surface band.[29] Taking into account the observed $\sqrt{3}$ LEED pattern, the (3×3) underlying symmetry revealed by ARUPS can be understood only if a (3×3) pattern exists locally. The behavior found for Sn/Si(111) is similar to the features of the parent system Sn/Ge(111).[12] In the case of Sn/Ge(111), the observation of a (3×3) structure by LEED allowed us to interpret the band splitting more easily as the result of the existence of two kinds of Sn atoms. The results found now for Sn/Si(111) are similar, and they lead also to the idea that there are two kinds of Sn atoms in Sn/Si(111) in a wide range of temperatures. This model is supported by core-level studies,[25,26] which show the existence of two components in the Sn $4d$ core level, both at LT and RT. However, there is no apparent stabilization of (3×3) long-range order at LT. A (3×3) background at LT has been observed in LEED (Ref. 25) and reflection high-energy electron diffraction[27] (RHEED), but a concomitant STM analysis[27] failed to observe any (3×3) periodicity and attributed the background to the existence of local defects randomly distributed, producing a short-range (3×3) perturbation.[37] It was claimed that defects, or maybe other effects, could possibly explain the two components observed in the Sn core level. In the case of ARUPS, however, we argue that the local (3×3) pinning produced by random defects can hardly produce a (3×3) ordering giving rise to a (3×3) reciprocal space band dispersion. Thus, the two components in the Sn core level and the split surface-state band must come from the existence at the surface of a well-ordered array of two different kinds of Sn atoms. Furthermore, the shape and occupation of the two split bands agree well with the predic-

tions for Sn/Si(111).[29] Besides these effects, theoretical calculations predict no phase transition for Sn/Si(111),[19] but a wide temperature range where vertical fluctuations with local (3×3) symmetry would be significant. Since the photoemission process is very fast, it provides a snapshot of the surface in a fs time scale.[37] In this time range both two-core-level components and a split surface band would be found. The existence of surface vibrations at RT that are frozen at LT has been confirmed by a recent study,[20] which found a soft surface phonon related to the (3×3) periodicity. This is a direct evidence of the model. The different Sn $4d$ core-level line shape for Sn/Ge(111) (Refs. 12 and 13) and Sn/Si(111) (Ref. 25) has prompted studies on the possible existence of a 2U phase for any of these systems.[31] Our results refer only to the surface electronic structure, but there should be a correlation between the number of Sn atoms in up position and the surface-state filling. Indeed, recent calculations for Sn/Ge(111) show that the 2U structure is semiconducting and exhibits a much smaller splitting between the two occupied surface bands.[31] The band structure found by us (see Fig. 4) cannot be described by the 2U theoretical bands. Indeed, it is fairly similar to the band structure of Sn/Ge(111)-(3×3). Thus, while there is a clear difference in the core-level line shape for both surfaces, the electronic band structure is similar and it is well described in both cases by the 1U model.

B. $Si_xSn_{(1-x)}$/Si(111)−($\sqrt{3}\times\sqrt{3}$)$R30°$ phase

An interesting question is the evolution of the electronic structure with Sn coverage in the stability range of the $\sqrt{3}$ structure. Figure 5 (top) shows spectra taken at normal emission as a function of Sn coverage with $h\nu=12.5$ eV at 170 K. We note that all of them exhibit a significant intensity. At this reciprocal space location ($\overline{\Gamma}$), it can be attributed to (3×3) band folding only. If this intensity indeed had (3×3) origin, it would be reasonable to expect the maximum normalized intensity at the ideal coverage of 0.33 ML where the intermixing of Si and Sn is minimum. To check this hypothesis we represent in Fig. 5 (bottom) the intensity integrated around the peak maximum as a function of the coverage. We do find that the maximum intensity lies around the ideal coverage, decreasing rapidly for higher coverages. This behavior confirms the (3×3) electronic origin of the surface state at $\overline{\Gamma}$. It also supports the idea that there is no significant coverage-dependent charge transfer between Sn and Si atoms, since a change in the solid solution concentration still maintains the (3×3) periodicity, at least in the 0.23–0.33 ML range.

Figure 6 (top) shows in detail a series of selected normalized spectra taken at the $\overline{K}$ point, the bottom of the surface-state band, as a function of coverage with $h\nu=12.5$ eV at 170 K. Neither the line shape nor the BE of the surface-state peak changes significantly in the coverage range probed. However, it is known that Si adatoms preferentially occupy the dominant site in the (3×3) unit cell (forming a honeycomb structure) in this coverage range.[26] This evidence confirms that the surface behaves as a solid solution. Furthermore, the BE of the surface state is constant within experimental accuracy. This indicates that an image of fully

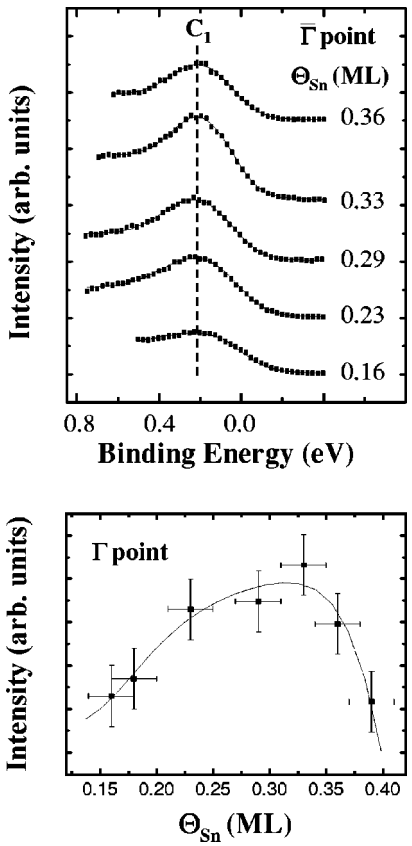

FIG. 5. Top: χ^2 line shape deconvolution of selected normalized photoemission spectra at the $\overline{\Gamma}$ point (dots), as a function of Θ_{Sn} ($h\nu=12.5$ eV, 170 K). The spectra have been fitted to a single component plus a background. The result of the fit appears as solid lines. Bottom: integrated surface-state intensity (binding energy range 0.0–0.40 eV) of the spectra in the top panel, as a function of Θ_{Sn}. The solid line is a guide to the eye.

decoupled surface states[30] is not correct, because in this case a shift of at least 0.25 eV would be found in the coverage range probed. We conclude that the dangling bonds of intermixed Si atoms behave in a way not much different from Sn dangling bonds and that the charge transfer between Si and Sn atoms is small in the 0.23–0.33 ML range.

Figure 6 (bottom) shows the $\overline{K}$-point-integrated intensity around the peak maximum (binding energy range 0.25–0.65 eV) of the dangling bond state as a function of Sn coverage. For coverages below $\sim$0.28 ML, the intensity of the surface state with higher BE is approximately constant, growing rapidly for larger coverages. For $\Theta\simeq0.23$ ML and in view of the site occupation sequence reported in Ref. 26, there are at least two Sn atoms per (3×3) unit cell. This suggests that the intensity increase for $\Theta>0.23$ ML is related to the appearance of long-range order in the structure and/or possibly to the formation of a $(2\sqrt{3}\times2\sqrt{3})R30°$ structure above 0.40 ML.[4]

We analyze in the following the metallic versus semiconducting character of the Sn/Si(111) interface as a function of coverage. For an ideal, flat $\sqrt{3}$ reconstruction, simple electron counting shows that the surface should be metallic, since there are seven valence electrons per unit cell. As Sn

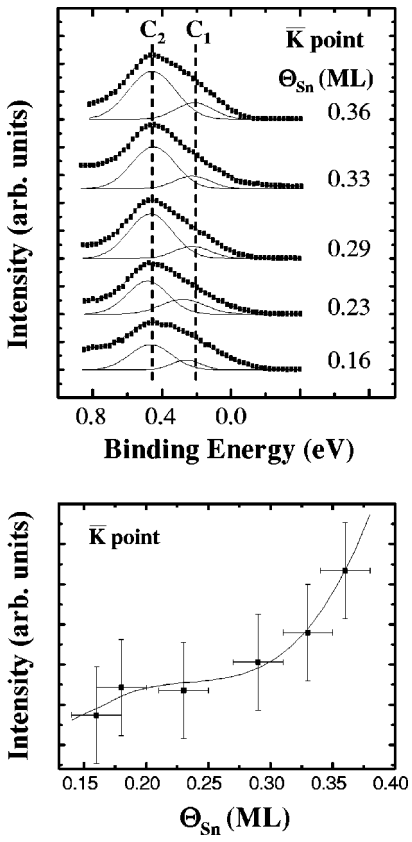

FIG. 6. Top: χ^2 line shape deconvolution of selected normalized photoemission spectra at the $\bar{K}$ point (dots) as a function of Θ_{Sn} ($h\nu = 12.5$ eV, 170 K). Solid lines represent the result of the fitting and the two components used (the background is not shown for clarity). Bottom: integrated intensity of the component C_2 (BE range 0.25–0.65 eV) of the top spectra as a function of Θ_{Sn}. The solid line is a guide to the eye.

coverage decreases and we get closer to the γ phase, nothing should change in principle, because intermixed Si atoms are also tetravalent and share the same electronegativity. However, theoretical calculations using a first-principles density-functional-theory local-density-approximation (DFT-LDA) tight-binding molecular dynamics technique[21] predict a different behavior. In the relaxed surface structure, Sn atoms appear slightly higher than Si atoms, which favors the transfer of charge from Si to Sn atoms. This gives rise to the opening of a surface band gap, and the surface becomes semiconducting for $\Theta_{Sn} = 0.16$ ML (γ phase). These predictions are supported by inverse photoemission results.[21]

Photoemission spectroscopy probes the occupied electronic valence band states. We find that the α phase is indeed metallic (see Fig. 4). It exhibits a prominent surface-state band that disperses rapidly to cross the Fermi energy close to the $\bar{M}_{(3\times3)}$ points. The photoemission intensity at the Fermi energy can be analyzed as a function of coverage. This photoemission intensity is a measurement of the density of states at the Fermi energy, and thus it should be sensitive to the metallic versus semiconducting character of the surface. To study this point we have performed a quantitative measurement of the photoemission intensity in a narrow

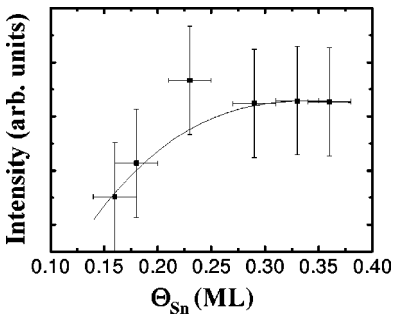

FIG. 7. Integrated photoemission intensity around the Fermi energy (binding energy window: ± 200 meV) as a function of the Sn coverage for a parallel momentum range between -0.1 and 0.8 Å^{-1} along the $\bar{\Gamma}\bar{K}$ direction, with $h\nu = 12.5$ eV at 170 K. The solid line is a guide to the eye.

(± 200 meV) window around the Fermi energy and afterwards integrated direction in a parallel momentum range from -0.1 to 0.8 Å^{-1} for each coverage studied (between 0.16 and 0.36 ML). The result is shown in Fig. 7. Before the integration (not shown), we have detected that the highest intensity at the Fermi energy (which corresponds to the Fermi momentum) remains at approximately the same value for a coverage range between 0.23 and 0.33 ML, while the Fermi momentum is larger for both smaller (0.16 ML) and larger coverages (0.36 ML). After the intensity integration of Fig. 7, it can be seen that for coverages in the range of 0.16–0.22 ML the intensity grows steadily, while it seems to remain constant above ~ 0.23 ML. Interestingly, we detect a Fermi edge in the whole coverage range analyzed, indicating that the surface is always metallic. However, the intensity decrease below ~ 0.23 ML suggests that the system may become semiconducting at lower coverages. We conclude from the results of Fig. 7 and from the constant Fermi momentum that, at least in the 0.23–0.33 ML range, there is no significant charge transfer between Si and Sn atoms and the surface exhibits constant electronic properties. In this range, the system behaves as a true solid solution. The constant intensity at the Fermi energy supports the idea that both kinds of adatoms lie at the same height (no charge transfer). At lower coverages the reduced density of states at the Fermi energy suggests some degree of charge transfer. These experimental results confirm the intermediate semiconducting phase proposed in previous works.[21,30]

IV. CONCLUSIONS

The electronic band structure of $Si_xSn_{(1-x)}/Si(111)-(\sqrt{3}\times\sqrt{3})R30°$ has been analyzed using angle-resolved photoemission along the two high-symmetry directions. The two main features of the band structure are the existence of a surface band splitting, which survives even at RT, and a significant intensity at the $\bar{\Gamma}$ point, characteristic of a (3×3) surface band folding. We conclude that the occupied electronic bands reflect an underlying (3×3) symmetry that supports the existence of two kinds of Sn atoms at the surface and local (3×3) ordering. The coverage dependence of the surface-state line shape and BE at the $\bar{K}$ point does not sup-

port a decoupling of the Sn and Si surface-state bands, meaning that there is no significant charge transfer between Si and Sn atoms present in the solid solution in the 0.23–0.33 ML range. The existence of a semiconductor-to-metal transition has been investigated in detail. The interface was found to be metallic in the 0.16–0.36 ML range, but there is a significant Fermi surface intensity increase for coverages above 0.22 ML. Below 0.23 ML our data are compatible with an increased Si-Sn charge transfer and possibly a semiconducting phase.

V. ACKNOWLEDGMENTS

We acknowledge financial support from MCyT (Spain) under Grant No. BFM-2001-0244 and from Comunidad de Madrid (Spain) under Grant No. 07N/0022/2002. The experiments performed at HASYLAB were supported by the IHP, Contract No. HPRI-CT-1999-00040, of the European Commission.

[1] L.J. Brillson, Surf. Sci. Rep. **2**, 123 (1982).
[2] V.G. Lifshits, K. Oura, A.A. Saranin, and A.V. Zotov, in *Physics of Covered Solid Surfaces*, Landolt-Börnstein, New Series, Group III, Vol. 42 A, pt. 1, edited by H.P. Bonzel (Springer, Berlin, 2001).
[3] A. Mascaraque and E.G. Michel, J. Phys.: Condens. Matter **14**, 6005 (2002).
[4] T. Ichikawa, Solid State Commun. **46**, 827 (1983); Surf. Sci. **140**, 37 (1984).
[5] J.S. Pedersen, R. Feidenhans'l, M. Nielsen, K. Kjaer, F. Gery, and R.L. Johnson, Surf. Sci. **189/190**, 1048 (1987).
[6] J.M. Carpinelli, H.H. Weitering, E.W. Plummer, and R. Stumpf, Nature (London) **381**, 398 (1996).
[7] J.M. Carpinelli, H.H. Weitering, M. Bartkowiak, R. Stumpf, and E.W. Plummer, Phys. Rev. Lett. **79**, 2859 (1997).
[8] J. Slezák, P. Mutombo, and V. Cháb, Phys. Rev. B **60**, 13 328 (1999).
[9] K. Horikoshi, X. Tong, T. Nagao, and S. Hasegawa, Phys. Rev. B **60**, 13 287 (1999).
[10] A.V. Melechko, J. Braun, H.H. Weitering, and E.W. Plummer, Phys. Rev. Lett. **83**, 999 (1999); Phys. Rev. B **61**, 2235 (2000).
[11] A. Mascaraque, J. Avila, E.G. Michel, and M.C. Asensio, Phys. Rev. B **57**, 14 758 (1998).
[12] J. Avila, A. Mascaraque, E.G. Michel, M.C. Asensio, G. LeLay, J. Ortega, R. Perez, and F. Flores, Phys. Rev. Lett. **82**, 442 (1999).
[13] R.I.G. Uhrberg and T. Balasubramanian, Phys. Rev. Lett. **81**, 2108 (1998).
[14] A. Mascaraque, J. Avila, J. Alvarez, M.C. Asensio, S. Ferrer, and E.G. Michel, Phys. Rev. Lett. **82**, 2524 (1999).
[15] O. Bunk, J.H. Zeysing, G. Falkenberg, R.L. Johnson, M. Nielsen, M.M. Nielsen, and R. Feidenhans'l, Phys. Rev. Lett. **83**, 2226 (1999).
[16] J. Zhang, Ismail, P.J. Rous, A.P. Baddorf, and E.W. Plummer, Phys. Rev. B **60**, 2860 (1999).
[17] J. Ortega, R. Pérez, and F. Flores, J. Phys.: Condens. Matter **14**, 5979 (2002).
[18] J. Ortega, R. Pérez, and F. Flores, J. Phys.: Condens. Matter **12**, L21 (2000).
[19] R. Pérez, J. Ortega, and F. Flores, Phys. Rev. Lett. **86**, 4891 (2001).
[20] D. Farías, W. Kamiński, J. Lobo, J. Ortega, E. Hulpke, R. Pérez, F. Flores, and E.G. Michel, Phys. Rev. Lett. **91**, 016103 (2003).
[21] A. Charrier, R. Pérez, F. Thibaudau, J.M. Debever, J. Ortega, F. Flores, and J.M. Themlin, Phys. Rev. B **64**, 115407 (2001).
[22] C. Törnevik, M. Göthelid, M. Hammar, U.O. Karlsson, N.G. Nilsson, S.A. Flodström, C. Wigren, and M. Östling, Surf. Sci. **314**, 179 (1994).
[23] J.M. Nicholls, B. Reihl, and J.E. Northrup, Phys. Rev. B **35**, 4137 (1987).
[24] S.T. Jemander, N. Lin, H.M. Zhang, R.I.G. Uhrberg, and G.V. Hansson, Surf. Sci. **475**, 181 (2001).
[25] R.I.G. Uhrberg, H.M. Zhang, T. Balasubramanian, S.T. Jemander, N. Lin, and G.V. Hansson, Phys. Rev. B **62**, 8082 (2000).
[26] L. Ottaviano, G. Profetta, L. Petaccia, S. Santucci, and M. Pedio, Surf. Sci. **501**, L171 (2002); Surf. Rev. Lett. **9**, L171 (2002).
[27] H. Morikawa, I. Matsuda, and S. Hasegawa, Phys. Rev. B **65**, 201308 (2002).
[28] M. Göthelid, M. Björkqvist, T.M. Grehk, G. Le Lay, and U.O. Karlsson, Phys. Rev. B **52**, R14 352 (1995).
[29] A. Charrier, R. Pérez, F. Thibaudau, J.-M. Debever, J. Ortega, F. Flores, and J.-M. Themlin, J. Phys.: Condens. Matter **22**, L521 (2001).
[30] G. Profeta, L. Ottaviano, S. Santucci, and A. Continenza, Phys. Rev. B **66**, 081303 (2002).
[31] G. Ballabio, G. Profeta, S. de Gironcoli, S. Scandolo, G.E. Santoro, and E. Tosatti, Phys. Rev. Lett. **89**, 126803 (2002).
[32] R.I.G. Uhrberg, G.V. Hansson, J.M. Nicholls, P.E.S. Persson, and S.A. Flodstrom, Phys. Rev. B **31**, 3805 (1985).
[33] T. Kinoshita, S. Kono, and T. Sagawa, Phys. Rev. B **34**, 3011 (1986).
[34] J. Lobo, A. Tejeda, A. Mugarza, and E.G. Michel, J. Vac. Sci. Technol. A **2**, 1298 (2003).
[35] The C_1 component is needed in the fit for most of the angular range probed (see Figs. 3 and 4). We did not include in Fig. 4 BE's closer to the Fermi energy than our energetic resolution, since the BE of the component C_1 does not represent the actual BE of the surface state.
[36] K. Würde, P. Krüger, A. Mazur, and J. Pollmann, Surf. Rev. Lett. **5**, 105 (1998).
[37] The question why the (3×3) phase does not manifest itself with STM at 6 K is still under discussion. Possible artifacts related to the measurement should be considered. Indeed, it has been recently reported that the apparent observation of symmetric dimers at very low temperatures (<10 K) in the closely related Si(100) system is due to the STM imaging mechanism (Ref. 38).
[38] Masanori Ono, A. Kamoshida, N. Matsuura, E. Ishikawa, T. Eguchi, and Y. Hasegawa, Phys. Rev. B **67**, 201306 (2003).